Food-grade TiO2 is trapped by intestinal mucus in vitro but does not impair mucin O-glycosylation and short-chain fatty acid synthesis in vivo: implications for gut barrier protection

Pauline Talbot, Joanna M. Radziwill-Bienkowska, Jasper B.J. Kamphuis, Karine Steenkeste, Sarah Bettini, Véronique Robert, Marie-Louise Noordine, Camille Mayeur, Eric Gaultier, Philippe Langella, et al.

HAL Id: hal-02624418

https://hal.inrae.fr/hal-02624418

Submitted on 26 May 2020

RESEARCH

CrossMark

Food-grade TiO$_2$ is trapped by intestinal mucus in vitro but does not impair mucin *O*-glycosylation and short-chain fatty acid synthesis in vivo: implications for gut barrier protection

Pauline Talbot[1], Joanna M. Radziwill-Bienkowska[2], Jasper B. J. Kamphuis[3], Karine Steenkeste[4], Sarah Bettini[3], Véronique Robert[1], Marie-Louise Noordine[1], Camille Mayeur[1], Eric Gaultier[3], Philippe Langella[1], Catherine Robbe-Masselot[5], Eric Houdeau[3], Muriel Thomas[1] and Muriel Mercier-Bonin[3]*

Abstract

Background: Titanium dioxide (TiO$_2$) particles are commonly used as a food additive (E171 in the EU) for its whitening and opacifying properties. However, the risk of gut barrier disruption is an increasing concern because of the presence of a nano-sized fraction. Food-grade E171 may interact with mucus, a gut barrier protagonist still poorly explored in food nanotoxicology. To test this hypothesis, a comprehensive approach was performed to evaluate in vitro and in vivo interactions between TiO$_2$ and intestinal mucus, by comparing food-grade E171 with NM-105 (Aeroxyde P25) OECD reference nanomaterial.

Results: We tested E171-trapping properties of mucus in vitro using HT29-MTX intestinal epithelial cells. Time-lapse confocal laser scanning microscopy was performed without labeling to avoid modification of the particle surface. Near-UV irradiation of E171 TiO$_2$ particles at 364 nm resulted in fluorescence emission in the visible range, with a maximum at 510 nm. The penetration of E171 TiO$_2$ into the mucoid area of HT29-MTX cells was visualized in situ. One hour after exposure, TiO$_2$ particles accumulated inside "patchy" regions 20 μm above the substratum. The structure of mucus produced by HT29-MTX cells was characterized by MUC5AC immunofluorescence staining. The mucus layer was thin and organized into regular "islands" located approximately 20 μm above the substratum. The region-specific trapping of food-grade TiO$_2$ particles was attributed to this mucus patchy structure. We compared TiO$_2$-mediated effects in vivo in rats after acute or sub-chronic oral daily administration of food-grade E171 and NM-105 at relevant exposure levels for humans. Cecal short-chain fatty acid profiles and gut mucin *O*-glycosylation patterns remained unchanged, irrespective of treatment.

Conclusions: Food-grade TiO$_2$ is trapped by intestinal mucus in vitro but does not affect mucin *O*-glycosylation and short-chain fatty acid synthesis in vivo, suggesting the absence of a mucus barrier impairment under "healthy gut" conditions.

Keywords: Food-grade TiO$_2$, Gut barrier, Mucin *O*-glycans, Mucus, Short-chain fatty acids

---

*Correspondence: muriel.mercier-bonin@inra.fr
[3] Toxalim (Research Centre in Food Toxicology), Université de Toulouse, INRA, ENVT, INP-Purpan, UPS, Toulouse, France
Full list of author information is available at the end of the article

Talbot *et al. J Nanobiotechnol* (2018) 16:53

Page 2 of 14

Background

Titanium dioxide (TiO_2) is widely used as a white pigment and opacifying agent, due to its brightness and high refractive index. It accounts for 70% of the world's pigment production, with 5000 metric tons produced per year, expected to rise to 60,000 metric tons by 2025. It is used in the food industry in an ultrafine form as a white coloring agent [referred to as food-grade additive E171 in the European Union (EU)] for confectionery, sauces, cakes, and pastries. In the United States, the Food and Drug Administration (FDA) approved the use of food-grade TiO_2 in 1966 with the stipulation that TiO_2 should not exceed 1% by weight of the food [1]. In Europe, EU Directive 94/36/EC authorizes the use of E171 in foodstuffs, without establishment of acceptable daily intake by the Joint Food and Agriculture Organization (FAO)/World Health Organization (WHO) Expert Committee on Food Additives, because intestinal TiO_2 absorption was considered to be very low [2]. A sizable fraction of nano-sized particles (primary particle size < 100 nm) is produced during the manufacturing process of the powder, accounting for 17–55% of the particles present, depending on the commercial supplier of E171 [3–6]. Consumption has been estimated to be 1–2 mg TiO_2/kg body weight (bw)/day for US children under 10 years of age, and 0.2–0.7 mg TiO_2/kg bw/day for other US consumers [3]. More recent exposure estimates have ranged between 0.2 and 0.4 mg/kg bw/day in infants and the elderly, and 5.5 and 10.4 mg/kg bw/day in children, depending on the exposure scenario [7].

To date, most data concerning the consequences of TiO_2 exposure on intestinal barrier function have been obtained in vitro using enterocyte-like cell models [8–15], hence bypassing the mucus layer. However, an increasing body of evidence suggests that mucus plays a key role in gut barrier homeostasis and host protection [16]. Mucus is on the front line, acting in concert with the intestinal epithelium and microbiota, to provide physical, biological, and chemical barriers to potentially harmful food particles [17–20]. However, mucus has only sporadically been taken into account when considering the fate of nanoparticles in the gut, as recently reviewed [21, 22]. In particular, there is only limited information concerning TiO_2 and oro-gastrointestinal mucus [6, 23–25], even though TiO_2 nanoparticles were first shown to stimulate mucin secretion by human ChaGo-K1 bronchial epithelial cells in the airways [26]. Porcine mucosa has been used as an ex vivo model for the oral cavity [24, 25], whereas Caco-2/HT29-MTX mucus-producing co-culture has been used to mimic gut-like conditions in vitro [6, 23]. Finally, the interactions between TiO_2 nanoparticles and mucus have been primarily characterized using standard nano-sized particles (TiO_2-NP) [23–25], despite

their size (primary size and percentage of nano-sized particles) and physico-chemical properties (crystalline structure, surface chemical composition, specific surface area, isoelectric point and agglomeration) which are quite different from those of food-grade TiO_2 [4, 27]. The sole exception has been the recent study of Dorier et al. [6] on E171.

We performed a mucus-targeted study using food-grade TiO_2 (E171) in comparison with the NM-105 (Aeroxyde P25) OECD (Organisation for Economic Cooperation and Development) reference nanomaterial. The TiO_2-trapping properties of mucus were evaluated for E171 using an in vitro approach with mucus-secreting HT29-MTX intestinal epithelial cells. We also compared the TiO_2-mediated effects in vivo in rats after acute (1-week) or sub-chronic (60 days) oral daily administration of E171 vs. NM-105 at relevant exposure levels for humans (0.1 and 10 mg/kg body weight (bw)/day). We focused on (i) cecal short-chain fatty acids, which were previously shown to be involved in the regulation of intestinal mucin MUC2 expression [28], and (ii) mucin *O*-glycosylation, because it influences the cohesive properties of mucus and hence its protective function [20].

Methods

Particle preparation

The E171 sample, obtained from a French commercial supplier of food coloring, was of the same batch as that used in the study of Bettini et al. [5]. NM-105 nanomaterial (also referenced as JRCNM01005a) was provided by the European Union Joint Research Centre (EU JRC) as a test material of manufactured TiO_2 nanoparticles (Aeroxyde P25) and selected by the OECD for safety evaluation of titanium-based nanomaterials. It displays mixed crystallinity, with anatase as the predominant form (85% anatase:15% rutile), and a primary particle diameter of 22 ± 1 nm [29]. The TiO_2 products were prepared according to the generic Nanogenotox dispersion protocol described by Jensen et al. [30]. Briefly, a 2.56 mg/mL stock suspension was prepared by pre-wetting the powder in absolute ethanol, followed by dispersion in a 0.05% (w/v) bovine serum albumin (BSA) solution and probe sonication on ice for 27 min at 40% amplitude (Sonifier Cell Disruptor Model 250 20 kHz, Branson Ultrasonics Corporation). The stock suspensions were always prepared fresh prior to each experiment, sonicated, and diluted to the target test concentrations with MilliQ-grade water.

Particle characterization

The hydrodynamic diameter and polydispersity index of the TiO_2 particles after the dispersion protocol were measured for E171 and NM-105 at a concentration of

Talbot *et al. J Nanobiotechnol* (2018) 16:53

Page 3 of 14

40 μg/mL in Milli-Q grade water by Dynamic Light Scattering (DLS, Zetasizer μV, Malvern Instruments Ltd., UK). Their global electrical surface properties were also assessed by measuring electrophoretic mobility (EM), which corresponds to the velocity of suspended particles under the influence of an applied electrical field. EM was measured in 1 mM KNO_3 with an automated laser zetameter (Zetaphoremetre II, CAD Instruments, France) under a 100-V electric field. The pH of the suspension was adjusted to between 2 and 7 by adding either nitric acid (HNO_3, Sigma-Aldrich) or potassium hydroxide (KOH, Sigma-Aldrich). The results are based on an automated video analysis of approximately 200–300 particles for each measurement. The mean velocity of the E171 and NM-105 TiO_2 particles was determined and expressed as EM in 10^{-8} m^2/s/V.

Cell culture

The HT29-MTX mucus-secreting subpopulation of the human colon carcinoma cell line HT29 [31] was kindly provided to the Micalis Institute (MT) by Dr. Thécla Lesuffleur (INSERM UMR S 938, Paris, France). Cells were routinely grown in Dulbecco's modified Eagle's minimal essential medium (DMEM) with 4.5 g/L glucose (Lonza, Verviers, Belgium), supplemented with 10% (v/v) fetal calf serum (FCS) (Lonza) inactivated for 1 h at 56 °C, 1% (v/v) L-Glutamine 200 mM (Lonza), and 1% (v/v) penicillin 10,000 U/mL-streptomycin 10,000 μg/mL (Lonza). Cells were seeded at a concentration of 1.2×10^5 cells/mL in μ-Slide 8-well glass bottom slides (Ibidi Biovalley, Nanterre, France) or on glass coverslips placed in 24-well tissue culture plates (Thermo Fisher Scientific—Nunc A/S, Waltham, MA USA) for time-lapse microscopy and fluorescent staining, respectively. Fully differentiated cells were obtained 21 days post-seeding [32]. Cells were maintained at 37 °C in a 10% CO_2:90% air atmosphere and the culture medium changed daily.

Fluorescent staining of mucus secreted by HT29-MTX cells

Fluorescent staining was performed as previously described [33] with several modifications. HT29-MTX cells were fixed with 4% paraformaldehyde (PFA) (ThermoFisher Scientific—Fisher Scientific, Waltham, MA USA) for 15 min at room temperature, washed three times with cold phosphate buffered saline (PBS), pH 7.5 (Lonza), and blocked for 90 min at room temperature with 3% (w/v) BSA (Sigma-Aldrich, St. Louis, MO, USA) in PBS. Two primary antibodies (Santa Cruz Biotechnology, Heidelberg, Germany) were used: rabbit anti-MUC5AC (H-160), as MUC5AC is the most prominent gel-forming mucin in this in vitro model [31] and mouse anti-E-cadherin (G-10) to visualize epithelial cells (tight junctions). Both were used overnight

at 4 °C at a 1:200 dilution each. Incubation with the secondary antibodies was carried out for 1 h at room temperature using 1:400 diluted anti-rabbit Alexa Fluor 647 and anti-mouse Alexa Fluor 555 goat antibodies (ThermoFisher Scientific—Invitrogen, Waltham, MA USA). After each incubation with antibody, HT29-MTX cells were washed 4 times with cold PBS for 10 min. Stained glass coverslips were mounted on Superfrost microscope slides (ThermoFisher Scientific—ThermoScientific, Waltham, MA USA) using ProLong Gold antifade reagent (Cat. No. P36930, ThermoFisher Scientific—Life Technologies, Waltham, MA USA) and examined on an Leica TCS SP8 AOBS inverted confocal microscope (Leica Microsystems, Mannheim, Germany) equipped with a motorized stage at the INRA MIMA2 platform (http://www.jouy.inra.fr/mima2/). Observations were performed with a 63 ×/1.40 N.A. oil immersion objective. Alexa Fluor 555 was excited at 561 nm using an argon laser and detected between 566 and 628 nm. Alexa Fluor 647 was simultaneously excited at 633 nm using a He/Ne laser and the emitted fluorescence recorded from 638 to 794 nm. Signals were recorded using hybrid detectors (HyD) in standard mode. Single 3D acquisitions were acquired at a scan speed of 600 Hz in bidirectional mode with a scanning zoom of 1, an image resolution of 1024×1024 pixels, a line average of 2, and for z-stacks, a z-step between each xy image of 0.3 μm. The images were analyzed, and graphical representations prepared using IMARIS 7.7.2 software (Bitplane, Zurich, Switzerland).

Confocal laser scanning microscopy of TiO_2 particles in contact with HT29-MTX cells

Visualization of TiO_2 particle distribution

The distribution of E171 vs. NM-105 TiO_2 particles at a concentration of 250 μg/mL around HT29-MTX cells was observed using a Leica TCS SP5 confocal laser scanning microscope (Leica Microsystems, France) located at the Centre de Photonique Biomédicale (CPBM) (Orsay, France). The autofluorescence of both cells and particles was excited at 364 nm with a continuous Argon laser and collected between 400 and 700 nm, using a 63× oil immersion objective with a 1.4 numerical aperture. The size of the images was 512×512 pixels. Z-stacks were recorded with a z-step of 1 μm from the substratum to the top of the biological structure. To discriminate between TiO_2 particles and HT29-MTX cells, spectra were reconstructed by imaging the epifluorescence on a photomultiplier with a 10-nm slit, which was moved by 3-nm steps. Spectral deconvolution was performed using the "Dye separation" process of the Leica acquisition software.

Talbot *et al. J Nanobiotechnol* (2018) 16:53

Page 4 of 14

Visualization of TiO₂ particle penetration as a function of time

Diffusive penetration of 250 µg/mL TiO_2 particles through the mucoid structure of HT29-MTX cells was measured by time-lapse microscopy using the same Leica TCS SP5 microscope, as previously described [34]. Briefly, the evolution of fluorescence intensity over time was observed in a focal plane located 18 µm above the glass surface to observe the mucus area. An x–y time series was initiated, in which images were collected every 30 s for 60 min, immediately after TiO_2 aqueous suspensions were very gently and homogeneously added to the medium above the cells. Images were analyzed using Leica software (Lite; Leica Microsystems, France). Simultaneous transmission imaging showed that no structural alteration of the cells occurred during this process.

Animals and experimental design

Adult male Wistar rats (175–200 g) were purchased from Janvier Labs (France) and housed in polypropylene cages under standard conditions (temperature 22 ± 2 °C and a 12-h light/dark cycle). Animals were allowed free access to food (standard pellets HARLAN 2018, Envigo RMS SARL, Gannat, France) and water. All experiments were approved by the Local Animal Care and Use Committee (TOXCOM-0036-EH–EH), in compliance with European directive 2010/63/UE. In the first series of experiments, rats were randomly divided into three groups, each containing eight animals, and dosed daily by intragastric gavage (200 µL) for 7 days with food-grade E171, NM-105 (10 mg/kg bw/day), or vehicle (water). In the second series of experiments, rats were randomly divided into three groups, each containing 10 animals, and exposed for 60 days to E171 at the same dose as in the previous experiment or a lower dose (0.1 mg/kg bw/day), through the drinking water, or water alone for the control animals. All rats were decapitated and the cecal contents collected for analysis of short-chain fatty acids and tissues from the small intestine and distal colon were sampled for mucin *O*-glycosylation.

Analysis of cecal short-chain fatty acids

The concentrations of short-chain fatty acids (SCFA), namely acetate, propionate, butyrate, valerate, caproate, isobutyrate, isovalerate, and isocaproate, were determined in the cecal contents by gas–liquid chromatography (Nelson 1020, Perkin-Elmer, St Quentin en Yvelines, France) as previously described [35]. SCFA concentrations are expressed in mM.

Analysis of gut mucin O-glycosylation

Jejunal and/or ileal and distal colonic mucosa were scraped and the mucins solubilized and purified by isopycnic density-gradient centrifugation (Beckman Coulter LE80K ultracentrifuge; 70.1 Ti rotor, $308,500 \times g$ at 15 °C for 72 h) [36]. The mucin-containing fractions were pooled, dialyzed into water, lyophilized, and further submitted to β-elimination under reductive conditions (0.1 M NaOH, 1 M KBH_4 for 24 h at 45 °C). Permethylation of the mixture of oligosaccharide alditols was carried out using the sodium hydroxide procedure. After derivation, the reaction products were dissolved in 200 µL methanol and further purified on a C18 Sep-Pak (Waters, Milford, MA). Permethylated oligosaccharides were analyzed by MALDI-TOF Mass Spectrometry (MS) in positive ion reflective mode as $[M+Na]^+$. The relative percentage of each oligosaccharide was determined based on the integration of peaks from the MS spectra.
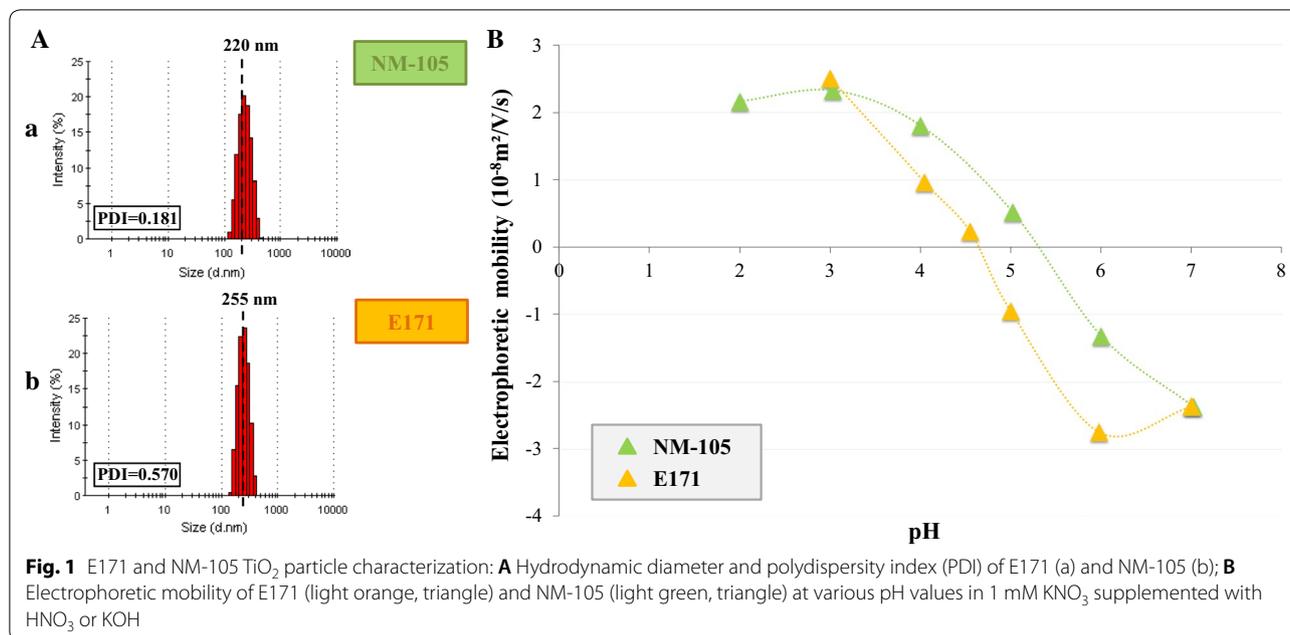
Results

Physicochemical characterization of food-grade (E171) vs. model (NM-105) TiO₂

The distribution of the hydrodynamic diameter after sonication for E171 and NM-105 TiO_2 particles suspended in Milli-Q grade water was determined by DLS. E171 had a mean hydrodynamic diameter of 255 nm and, under the same conditions, NM-105 exhibited a mean hydrodynamic diameter of 220 nm (Fig. 1A). This indicated that, in both cases, some agglomerates and/or aggregates remained in the suspension, given the primary TiO_2 particle size measured by transmission electron microscopy, i.e., 22 ± 1 nm (and 100% of particles below 100 nm in diameter) for NM-105 [29] and 118 ± 53 nm (and 44.7% of particles below 100 nm in diameter) for our E171 batch [5]. Figure 1B shows the electrophoretic mobility measurements recorded for E171 and NM-105 in 1 mM KNO_3 at discrete pH values ranging from 2 to 7. Both types of TiO_2 exhibited the typical pH-dependence of the electrophoretic mobility of metal oxides, and the isoelectric point (IEP) values for E171 and NM-105 were 4.6 and 5.3, respectively.

Penetration and localization of TiO₂ particles within HT29-MTX cells

In contrast to the NM-105 nanomaterial where no fluorescence emission was detected in the conditions under study, food-grade E171, once excited in the near-ultraviolet (UV) range at 364 nm, fluoresced in the visible range with a maximum at 510 nm in the culture medium (Fig. 3i). Based on these intrinsic fluorescence properties, we chose E171 for further time-lapse experiments to visualize the penetration of TiO_2 particles into the mucoid area of HT29-MTX cells in situ. We observed penetration of food-grade TiO_2 particles into the mucus and accumulation inside "patchy" regions by setting the focal plane 18 µm above

Talbot *et al. J Nanobiotechnol* (2018) 16:53

Page 5 of 14

Fig. 1 E171 and NM-105 TiO$_2$ particle characterization: **A** Hydrodynamic diameter and polydispersity index (PDI) of E171 (a) and NM-105 (b); **B** Electrophoretic mobility of E171 (light orange, triangle) and NM-105 (light green, triangle) at various pH values in 1 mM KNO$_3$ supplemented with HNO$_3$ or KOH

the substratum surface: fluorescence intensity inside some areas increased continuously over time, doubling within 1 h (area 1), whereas it remained almost unchanged in others (area 2) (Fig. 2). Such differences in fluorescence intensity likely indicate region-specific accumulation of TiO$_2$ particles. This preferential localization of TiO$_2$ particles was confirmed by z-stacks of fluorescence intensity images. Indeed, the only observable signal before E171 addition was cellular autofluorescence in the first micrometers (~ 15 μm) above the substratum (Additional file 1). In contrast, we observed fluorescence deeper, within patches, 1 h after E171 addition (Fig. 2 and Additional file 2). We recorded spectra at different z-positions to further characterize this fluorescence pattern (Fig. 3). Near the substratum, the spectrum displayed a maximum at 480 nm, similar to that for the cells alone, whereas 20 μm above the substratum (i.e., in the region of high fluorescence intensity), the spectrum was identical to that obtained with food-grade TiO$_2$ alone in the cell culture medium (Fig. 3i). The spectral images recorded in these different focal planes were then deconvoluted to separate the fluorescence of TiO$_2$ from that of the cells (Fig. 3b–d, f–h). The fluorescence near the substratum mainly originated from the cells, whereas in the upper layers it originated from the TiO$_2$ particles, which accumulated into "islands", while the surrounding medium contributed very little to global fluorescence (see the black background in Fig. 3f). TiO$_2$ accumulation was also visualized in the transmission images (Fig. 3a, e) as
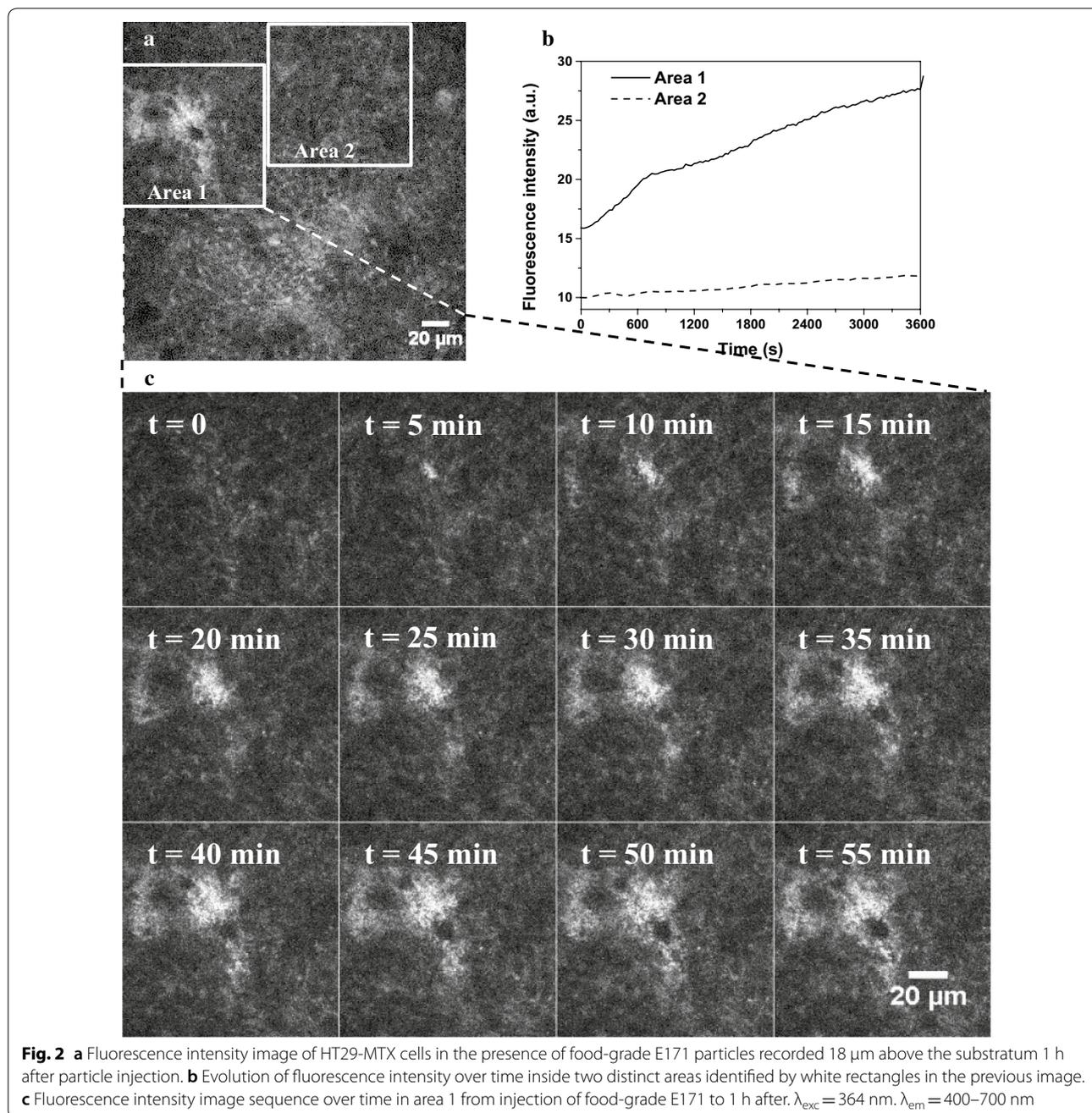
black shadows, because light cannot pass through TiO$_2$ particles.

We investigated the region-specific accumulation of E171 TiO$_2$ particles by characterizing the structure of the mucus produced by HT29-MTX cells by MUC5AC immunofluorescence staining followed by confocal laser scanning microscopy (Fig. 4). We observed a thin layer of mucus, with a thickness of less than 5 μm (Fig. 4B). Furthermore, this mucus layer did not homogenously cover the cells underneath, but was rather organized as regular "islands", located approximately 20 μm above the substratum (Fig. 4A, B), consistent with the TiO$_2$ accumulation pattern depicted above. Thus, the region-specific trapping of food-grade TiO$_2$ may be related to the patchy structure of the mucus, even though these fluorescence experiments do not provide direct experimental evidence.

TiO$_2$ oral exposure in rats: impact on cecal short-chain fatty acids and mucin *O*-glycosylation

We next evaluated TiO$_2$-mediated effects in vivo after oral exposure, depending on TiO$_2$ type (E171 vs. NM-105), treatment duration (1-week vs. sub-chronic 60 days), and the exposure level (0.1 mg/kg bw/day vs. 10 mg/kg bw/day). We focused on the synthesis of cecal short-chain fatty acids (SCFA) and gut mucin *O*-glycosylation.

A 7-day oral exposure of rats to TiO$_2$ had little to no impact on overall cecal composition of SCFA relative to controls, irrespective of TiO$_2$ type, E171 or NM-105

Talbot *et al. J Nanobiotechnol* (2018) 16:53

Page 6 of 14

Fig. 2 **a** Fluorescence intensity image of HT29-MTX cells in the presence of food-grade E171 particles recorded 18 µm above the substratum 1 h after particle injection. **b** Evolution of fluorescence intensity over time inside two distinct areas identified by white rectangles in the previous image. **c** Fluorescence intensity image sequence over time in area 1 from injection of food-grade E171 to 1 h after. $\lambda_{exc} = 364$ nm. $\lambda_{em} = 400–700$ nm

(Figs. 5a and 6a). There were also no significant differences relative to controls for acetate, propionate, butyrate (Fig. 5b), or other SCFAs (Fig. 6b) following sub-chronic oral exposure (60 days) with food-grade TiO_2 in the drinking water at doses of either 0.1 or 10 mg/kg bw/day, i.e., doses approximating human dietary levels for adults and children [3, 7]. In addition, there was no effect relative to controls on mucin *O*-glycosylation in the small intestine of the rats following 7- or 60-day TiO_2 oral

exposure, regardless of TiO_2 type (E171 and NM-105) or E171 dose tested (Fig. 7a, c). Indeed, there were no substantial modifications for neutral (the most abundant structures), sialylated, or sulfated oligosaccharides. The proportion of neutral *O*-glycans was lower in the colon of control animals than in the small intestine, which was associated with a higher amount of sialylated and sulfated structures (Fig. 7). There were also no TiO_2-induced changes in colonic *O*-glycans after either a 1-week or

Talbot *et al. J Nanobiotechnol* (2018) 16:53

Page 7 of 14

Fig. 3 a Transmission and **b** fluorescence intensity images of HT29-MTX cells in the presence of food-grade E171 particles close to the substratum. **c** Spectral image of cells/culture medium. **d** Spectral image of E171 particles derived from the deconvolution of the fluorescence intensity image recorded close to the substratum. **e–h** Same as for **a–d** for a focal plane located 24 μm from the substratum. **i** Normalized fluorescence emission spectra of TiO$_2$ particles in cell culture medium (green) and HT29-MTX cells alone in cell culture medium (red) or in the presence of TiO$_2$ particles 2 μm (black solid line) or 20 μm above the substratum (black dashed line). $\lambda_{exc} = 364$ nm. $\lambda_{em} = 400$–700 nm

sub-chronic treatment relative to control conditions (Fig. 7b, d).

Discussion

The whitening and opacifying properties of TiO$_2$ are commonly exploited when it is used as the food additive E171. However, the possibility of gut barrier disruption and/or an intestinal homeostatic imbalance (including microbiota dysbiosis) has been of increasing concern, due to the presence of a nano-sized fraction in this additive [4, 27]. Indeed, recent studies have reported adverse effects of in vitro exposure of intestinal epithelial cells to E171 [6, 11, 37] some of which possibly predispose the host to intestinal diseases and colorectal cancer, as shown in rodents [5, 38]. Intestinal mucus is still an underestimated gut target in food nanotoxicology [21, 22] and little data is currently available concerning the effects of TiO$_2$. Most available data have been generated using in vitro cell models, exclusively studying the effects of TiO$_2$ nanoparticles (TiO$_2$-NP) [23, 26].

Talbot *et al. J Nanobiotechnol* (2018) 16:53
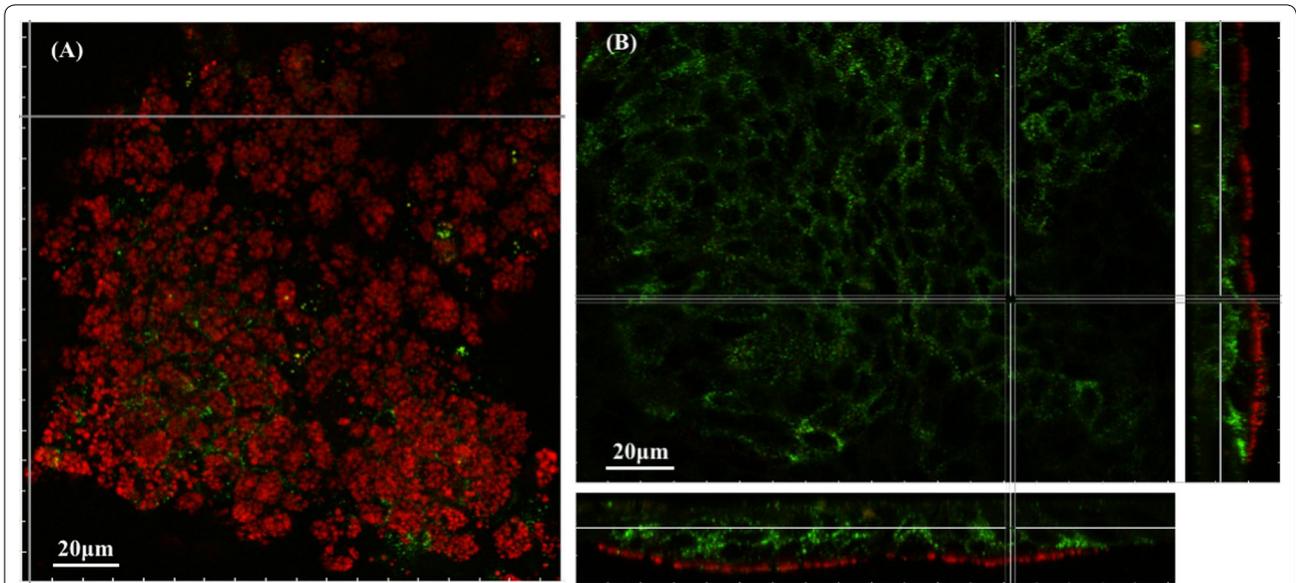
Page 8 of 14

Fig. 4 MUC5AC immunofluorescence staining of the HT29-MTX cell line. Representative confocal laser scanning microscopy z-stack image of MUC5AC (in red) produced by HT29-MTX cells (E-cadherin, in green) cultured under standard conditions. **A** z-stack section (x, y) at the level of the mucus; **B** z-stack section (x, y) at the level of HT29-MTX cells with orthogonal x (y, z) and y (x, z) sections on the right and bottom, respectively. The image was prepared using the easy 3D section view of IMARIS software with extended view (signal gathered from a thickness of 5 μm)
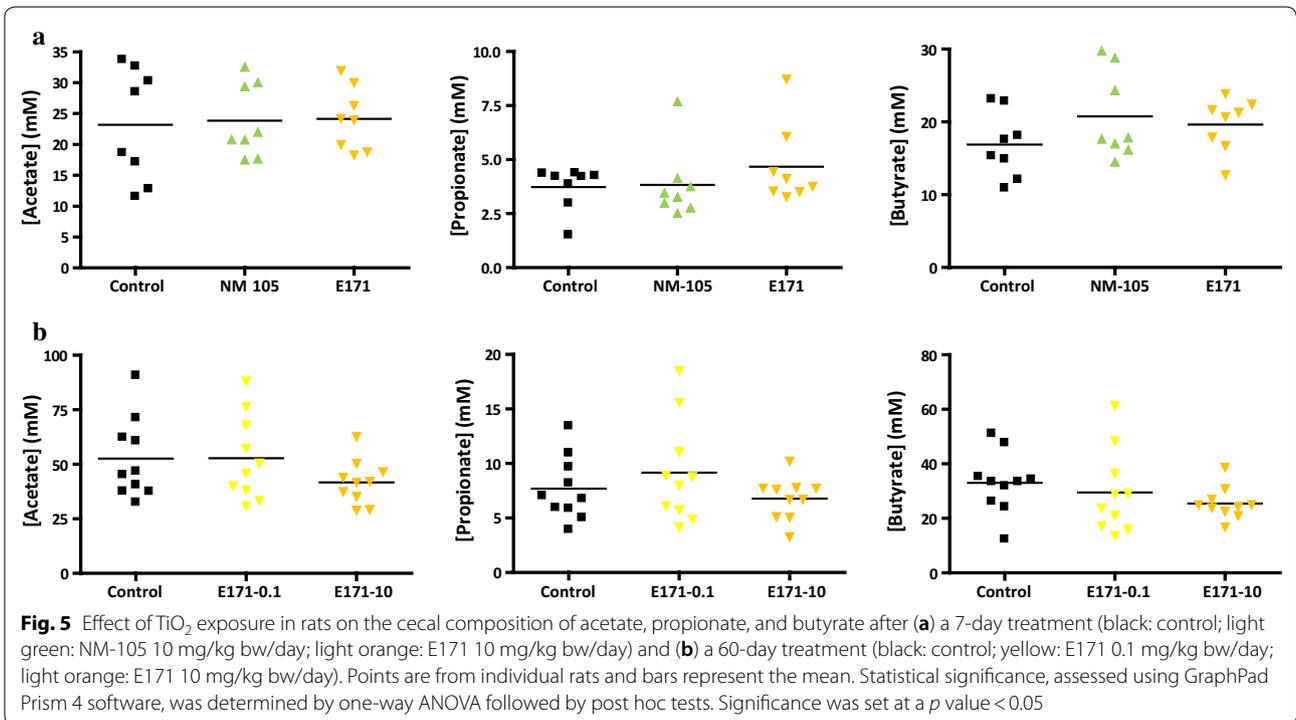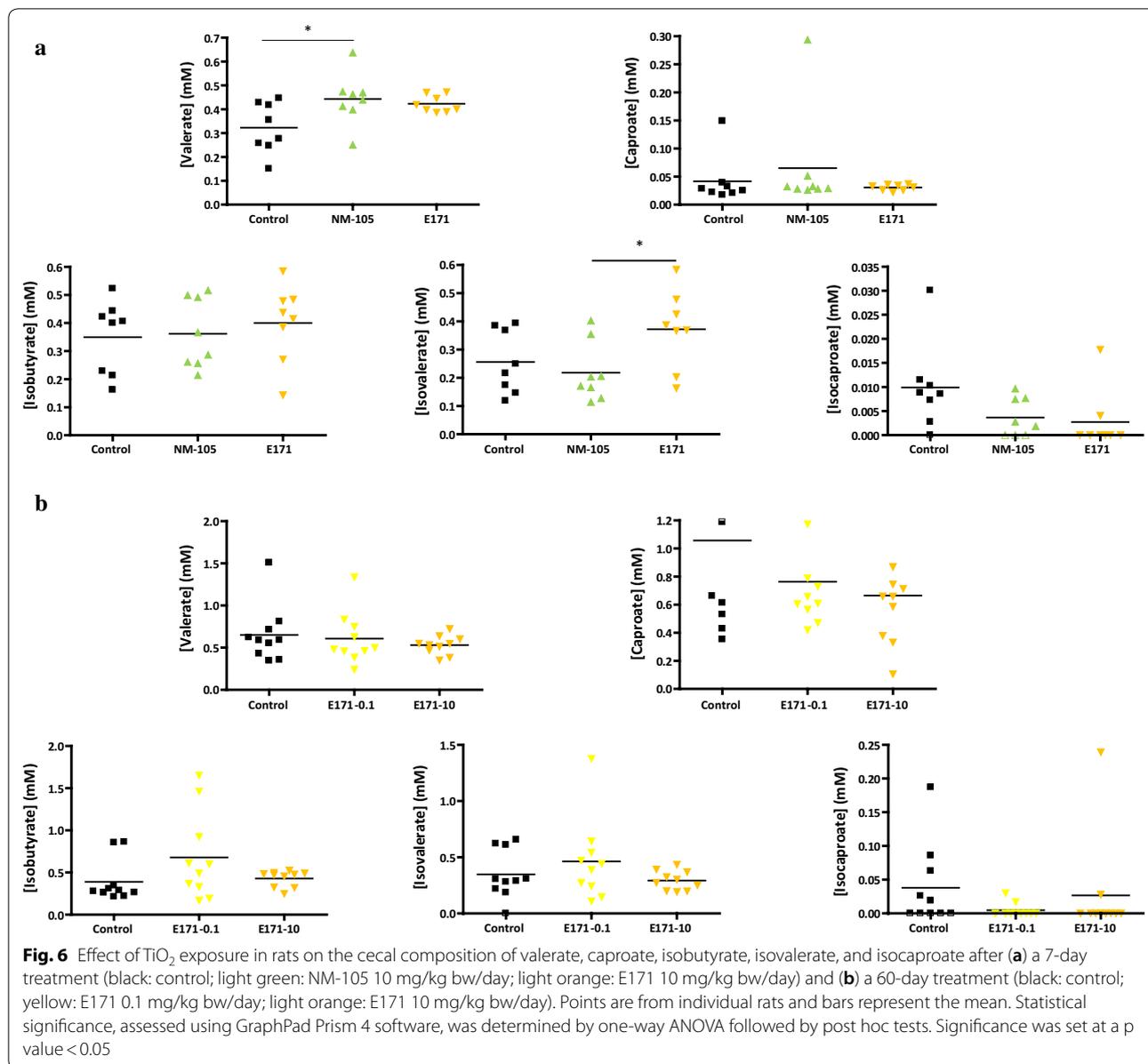

Fig. 5 Effect of TiO_2 exposure in rats on the cecal composition of acetate, propionate, and butyrate after (**a**) a 7-day treatment (black: control; light green: NM-105 10 mg/kg bw/day; light orange: E171 10 mg/kg bw/day) and (**b**) a 60-day treatment (black: control; yellow: E171 0.1 mg/kg bw/day; light orange: E171 10 mg/kg bw/day). Points are from individual rats and bars represent the mean. Statistical significance, assessed using GraphPad Prism 4 software, was determined by one-way ANOVA followed by post hoc tests. Significance was set at a *p* value < 0.05

Various profiles for the absorption and transport of TiO_2-NP have been described, depending on whether epithelial cells are cultured alone or with goblet cells [23]. Intrace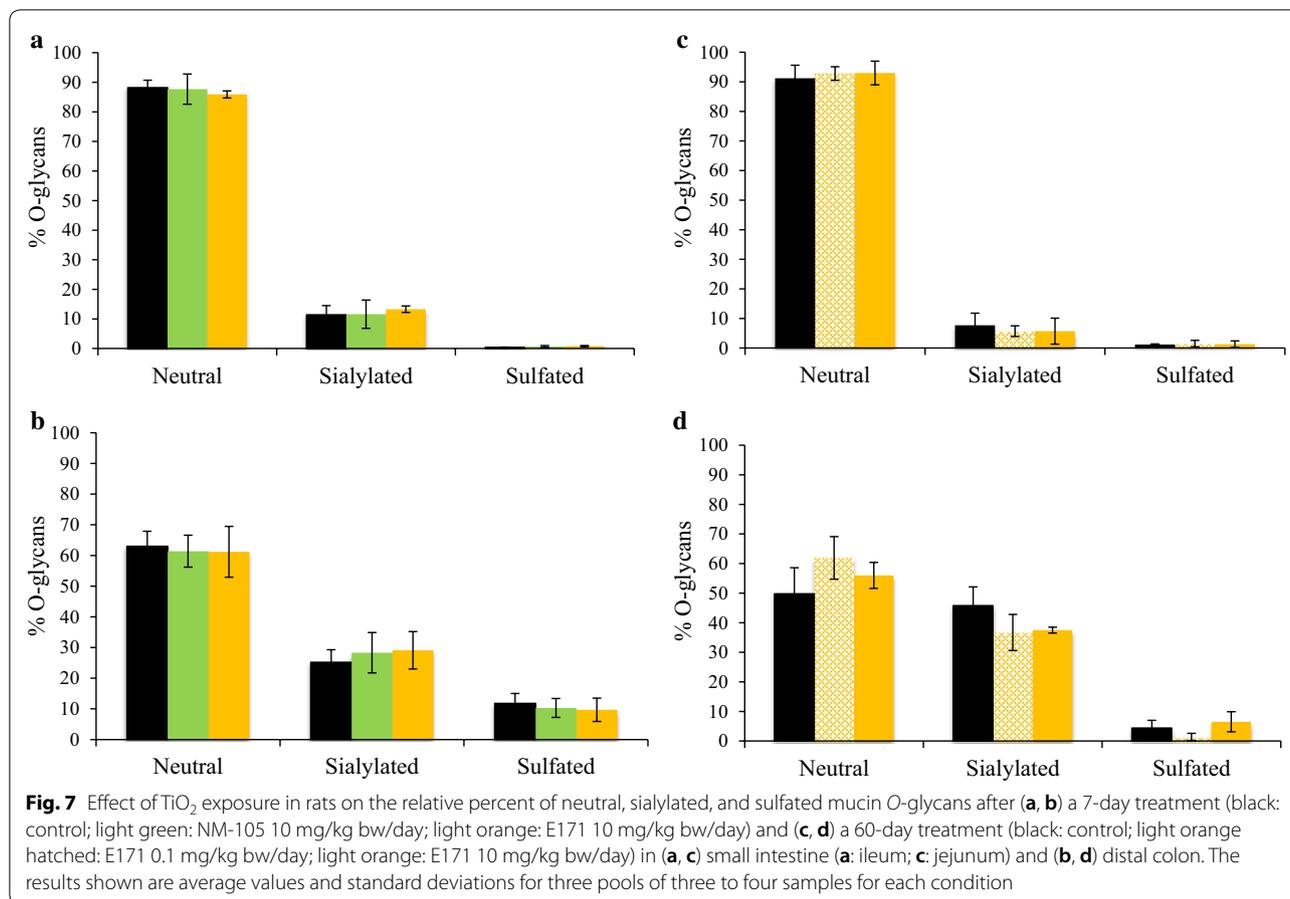llular TiO_2-NP accumulation has been mapped through Ti-distribution imaging by particle-induced X-ray emission. The authors showed that Caco-2 cells alone in monoculture displayed low levels of intracellular Ti accumulation after 24 h of contact. In contrast, the

Talbot *et al. J Nanobiotechnol* (2018) 16:53

Page 9 of 14

Fig. 6 Effect of TiO$_2$ exposure in rats on the cecal composition of valerate, caproate, isobutyrate, isovalerate, and isocaproate after (**a**) a 7-day treatment (black: control; light green: NM-105 10 mg/kg bw/day; light orange: E171 10 mg/kg bw/day) and (**b**) a 60-day treatment (black: control; yellow: E171 0.1 mg/kg bw/day; light orange: E171 10 mg/kg bw/day). Points are from individual rats and bars represent the mean. Statistical significance, assessed using GraphPad Prism 4 software, was determined by one-way ANOVA followed by post hoc tests. Significance was set at a p value < 0.05

same treatment in the presence of goblet cells (Caco-2/HT29-MTX mucus-producing co-culture) led to 50-fold higher levels of intracellular accumulation [23], suggesting facilitated translocation of TiO$_2$-NP in the presence of mucus. In contrast, another study using the same type of TiO$_2$-NP, but Inductively Coupled Plasma Mass Spectrometry (ICP-MS) to measure Ti content, showed that Ti accumulation in Caco-2 cells after 6 or 48 h of contact was slightly higher than in Caco-2/HT29-MTX cells; however, the differences were not statistically significant. The same results were obtained after repeated exposure for 21 days [6]. Ex vivo studies on porcine buccal mucosa also reported that TiO$_2$-NP were able to permeate the

mucus layer and penetrate the underlying tissue, regardless of their size and hydrophilicity/hydrophobicity [24, 25].

Physico-chemical analysis of E171 revealed a hydrodynamic diameter of 255 nm, which was of the same order of magnitude as values obtained for the same commercial source [5] and other food-grade TiO$_2$ samples [4], where effects of sonication protocols may influence the size of agglomerates [39]. E171 was also found to exhibit the typical pH-dependence of electrophoretic mobility of metal oxides, in contrast to the findings reported by Yang et al. [4] who observed little change in electrophoretic mobility as a function of pH for other food-grade TiO$_2$ sources.

Talbot *et al. J Nanobiotechnol* (2018) 16:53

Page 10 of 14

Fig. 7 Effect of TiO$_2$ exposure in rats on the relative percent of neutral, sialylated, and sulfated mucin *O*-glycans after (**a**, **b**) a 7-day treatment (black: control; light green: NM-105 10 mg/kg bw/day; light orange: E171 10 mg/kg bw/day) and (**c**, **d**) a 60-day treatment (black: control; light orange hatched: E171 0.1 mg/kg bw/day; light orange: E171 10 mg/kg bw/day) in (**a**, **c**) small intestine (**a**: ileum; **c**: jejunum) and (**b**, **d**) distal colon. The results shown are average values and standard deviations for three pools of three to four samples for each condition

Furthermore, the IEP value for E171 was 4.6. Yang et al. [4] found a variety of IEP values (i.e., from < 2.5 to 4.0) for five food-grade TiO$_2$ sources, whereas Dudefoi et al. [27] reported a narrow range between 4.0 and 4.2 for food-grade TiO$_2$ from other suppliers. These differences are probably due to the variable use of anionic phosphate-containing surfactants, as phosphate adsorbed to TiO$_2$ surfaces might decrease the IEP [4, 27]. Our food-grade TiO$_2$ was shown to be devoid of any surface coating with phosphate [5].

This is the first study to assess the interaction of food-grade TiO$_2$ with mucus by coupling in vitro and in vivo approaches. For our in vitro experiments on HT29-MTX cells, the chosen concentration was of the same order of magnitude as that used in the recent study of Dorier et al. [6] who analyzed the interactions of E171 with Caco-2/ HT29-MTX cells, in comparison with Caco-2 cells, during acute vs. repeated exposure. The authors reported that E171 accumulated more than P25 under both exposure scenarios, due to larger E171 agglomerates, which settled more quickly than those of the reference nanomaterial, leading to a higher level of cell exposure and cell response. They also concluded that E171 can cross

the mucus layer, which was roughly imaged using Alcian Blue staining, since the two cellular models with and without mucus accumulated similar amounts of TiO$_2$. Here, fluorescent staining with an anti-MUC5AC antibody and confocal microscopy enabled visualization of the mucus produced by HT29-MTX cells, as MUC5AC was shown to be the major gel-forming mucin in this in vitro model [31]. We showed that mucus did not form a uniform layer above the cell surface, but rather a patchy structure with a thickness of less than 5 μm. Even though mucus secreted by HT29-MTX cells has been described to form a dense gel layer, in some cases entirely covering the cell surface [40–42], our observations are in agreement with previous studies in which mucus patches were visualized instead [33, 43–45]. Here, we found that food-grade TiO$_2$ particles formed sparsely distributed clusters throughout the sample undoubtedly embedded in these mucus "islands". This confirms the in vitro barrier function of mucus against translocation of particles, mainly determined by their size, surface charge and surface hydrophobicity [21]. This is in contrast to the findings of Dorier et al. [6], but was already highlighted by Georgantzopoulou et al. [46] using a Caco-2/HT29-MTX

Talbot *et al. J Nanobiotechnol* (2018) 16:53

Page 11 of 14

co-culture and silver particles of similar size to the TiO_2 used in this study (200 nm).

We compared the TiO_2 mucus-related effects in rats after acute (1-week) or sub-chronic (60 days) oral daily administration of E171 vs. NM-105 at relevant exposure levels for humans (0.1 and 10 mg/kg bw/day). In vivo, mucus covers the intestinal epithelium but differently along the gastrointestinal tract. In particular, in rodents, mucus in the small intestine is single-layered and fills up the space between the villi and covers them, but is not attached to the epithelium and is penetrable to particles with the same size than that of bacteria [47]. In contrast, in the colon, a two-layered mucus system organization is generally described [48, 49]: the inner layer is densely packed, firmly attached to the epithelium, and devoid of bacteria, while the outer layer is movable, has an expanded volume and is heavily colonized by bacteria. However, Kamphuis et al. [50] recently proposed that the mucus layer in the distal colon of rodents covers the faeces instead of the epithelium. This faecal mucus layer confines the microbiota to the faeces and prevents it from remaining in empty distal colon. In the proximal colon, the mucus does not form a separating layer between bacteria and epithelium. These findings offer a new view of the mucus structure/function relationship. Besides its barrier properties, mucus is increasingly recognized to exert other key physiological functions essential for gut health. In particular, it provides a habitat for the gut microbiota since the wide diversity of mucin-derived carbohydrates can be utilized by bacteria as carbon sources [51–53] and/or preferential binding sites [54]. It was even suggested that such enormous repertoire could be at play in the region-specific colonization of bacteria in the gut [55]. Mucolytic bacteria, some of them being biomarkers in gut health and disease [56, 57], possess a large set of enzymes (glycosidases, sulphatases, sialidases…) to degrade mucin glycans and to harvest oligosaccharides for their own metabolism, thus conferring competitive advantage for mucosal surface colonization. Another important trait for adaptation of intestinal bacteria to the mucosal environment is their mucus-binding capacity, driven by specific determinants like pili and/or mucus-binding proteins in lactobacilli [58, 59].

Due to its trapping properties, mucus may act as a reservoir of TiO_2 particles, leading to areas with a high local concentration. Owing to the mucus/microbiota interplay in the gut, the gut microbiota may be affected because of the reported in vitro bacterial toxicity of nano-sized TiO_2 [60–62], and also food-grade E171 as recently shown by our group [63]. Indeed, there is growing evidence that the microbiota is a major player in food toxicology in the gut. Commensal bacteria have a capacity to metabolize xenobiotics and alter their toxicity to the host, as observed for

drugs. Xenobiotics may themselves alter bacterial populations that colonize the gut, leading to dysbiosis and associated chronic diseases [64–66]. The consequences of oral exposure to TiO_2 and other nanoparticles on the intestinal microbiota are largely unknown [21, 22, 67, 68]. Here, we focused on putative in vivo TiO_2-induced changes to the fermentation products (SCFA) of commensal bacteria, because their effects, especially those of butyrate, on mucin synthesis and mucus characteristics have been described in vitro, ex vivo, and in vivo [19, 28, 69–71]. In particular, butyrate, propionate, and acetate, have been shown to increase *MUC2* mRNA synthesis in the LS174T cell line [28]. Butyrate increased *MUC2* mRNA levels at low concentrations (1 mM) but had no effect at moderate and high concentrations (5–15 mM). Stimulation with low concentrations of butyrate (1–2 mM) also increased MUC2 protein synthesis [28]. On the other hand, as seen above, mucus is an important substrate for the intestinal microbiota, especially SCFA-producing members [72–74] and considerable changes in mucus production would therefore result in altered SCFA profiles. In our study, exposure to food-grade TiO_2 had little to no impact on the overall cecal composition of SCFA, including butyrate, irrespective of treatment duration (1-week vs. sub-chronic), suggesting that there were no substantial changes in mucus "quantity". We then focused on mucus "quality" by assessing mucin *O*-glycosylation. Neither 1-week or sub-chronic exposure to food-grade TiO_2 altered *O*-glycosylation of mucins from the small intestine and colon relative to untreated animals, first reinforcing the little impact on the "mucophilic" population of the gut microbiota. The only published study on the consequences of oral nanoparticle exposure to mucus deals with silver nanoparticles in rats [75]. Silver nanoparticle treatment resulted in a decrease in the level of neutral and acidic mucins in goblet cells, an increase in sialomucin levels, and a decrease in sulfomucin levels. We previously showed that changes in mucin *O*-glycan composition in rats may influence physico-chemical interactions and then condensation/bundling of mucin fibers, with a direct deleterious impact on the morphology and physical properties of the mucus network (i.e., loss in cohesive properties), and hence its protective barrier function [20]. In our study, the absence of mucin *O*-glycan alterations indicates that the protective function of mucus against particle uptake probably remained intact, even after sub-chronic oral exposure to food-grade TiO_2.

Conclusions

This study used a comprehensive approach to evaluate interactions between food-grade TiO_2 (E171 additive) and intestinal mucus. Results were compared with those

Talbot *et al. J Nanobiotechnol* (2018) 16:53

Page 12 of 14

of the NM-105 (Aeroxyde P25) OECD reference nano-material. We showed region-specific trapping of food-grade TiO_2 particles by mucus-secreting HT29-MTX intestinal epithelial cells, likely due to the patchy structure of mucus in this in vitro model. Cecal short-chain fatty acid profiles and mucin *O*-glycosylation patterns in the small intestine and colon were unchanged for E171 and also NM-105 after acute (1-week) and sub-chronic (60 days) oral exposure of rats at relevant exposure levels for humans (0.1 and 10 mg/kg body weight (bw)/day), suggesting the absence of a mucus barrier impairment under these "healthy gut" conditions. However, the protective functions of mucus are not static, as alterations in mucus production and composition have been shown to occur in response to microbial challenge, variations in diet, and intestinal disorders. These factors might influence the effects of the food additive E171. It should thus be informative to evaluate the risks of food-grade TiO_2 uptake specifically in situations in which the intestinal barrier function is defective, in particular an impaired mucus barrier.

Additional files

Additional file 1. Movie sequence showing the fluorescence distribution inside HT29-MTX structures from the substratum to the top before the addition of food-grade TiO_2 (E171).

Additional file 2. Movie sequence showing the fluorescence distribution inside HT29-MTX structures from the substratum to the top 1 hour after the addition of food-grade TiO_2 (E171).

Abbreviations

BSA: bovine serum albumin; CPBM: Centre de Photonique Biomédicale; DLS: Dynamic Light Scattering; DMEM: Dulbecco's modified Eagle's minimal essential medium; EM: electrophoretic mobility; EU: European Union; EU JRC: European Union Joint Research Centre; FAO: Food and Agriculture Organization; FDA: Food and Drug Administration; FCS: fetal calf serum; HNO_3: nitric acid; HyD: hybrid detectors; ICP-MS: Inductively Coupled Plasma Mass Spectrometry; IEP: isoelectric point; KOH: potassium hydroxide; MS: Mass Spectrometry; OECD: Organisation for Economic Cooperation and Development; PFA: paraformaldehyde; PBS: phosphate buffered saline; SCFA: short-chain fatty acids; TiO_2: titanium dioxide; TiO_2-NP: TiO_2 nanoparticles; UV: ultraviolet; WHO: World Health Organization.

Authors' contributions

EH, PL, MT and MMB conceived and designed the study. PT, JMRB and VR performed in vitro experiments. PT, MMB and KS performed and analyzed confocal laser scanning microscopy experiments. SB, EG and EH performed in vivo experiments. CRM analyzed gut mucin *O*-glycosylation. CM and MLN analyzed cecal short-chain fatty acids. MMB, JBJK, JMRB, KS, CRM, EH and MT wrote the manuscript; all authors contributed to the discussion. All authors read and approved the final manuscript.

Author details

[1] Micalis Institute, INRA, AgroParisTech, Université Paris-Saclay, 78350 Jouy-en-Josas, France. [2] Institute of Biochemistry and Biophysics, Polish Academy of Sciences, Pawinskiego 5A, 02-106 Warsaw, Poland. [3] Toxalim (Research Centre in Food Toxicology), Université de Toulouse, INRA, ENVT, INP-Purpan, UPS, Toulouse, France. [4] Institut des Sciences Moléculaires d'Orsay (ISMO), CNRS, Université Paris-Sud, Université Paris-Saclay, Orsay, France. [5] Univ. lille, CNRS, UMR8576-UGSF-Unité de Glycobiologie Structurale et Fonctionnelle, F59000 Lille, France.

References

1. Joint FAO/WHO Expert Committee on Food Additives. Combined compendium of food additive specifications. Rome: Food and Agriculture Organization of the United Nations; 2006.
2. EFSA Panel on Food Additives and Nutrient Sources Added to Food. Opinion of the Scientific Panel on food additives, flavourings, processing aids and materials in contact with food (AFC) on Titanium dioxide. EFSA J. 2005;3:163.
3. Weir A, Westerhoff P, Fabricius L, Hristovski K, von Goetz N. Titanium dioxide nanoparticles in food and personal care products. Environ Sci Technol. 2012;46:2242–50.
4. Yang Y, Doudrick K, Bi X, Hristovski K, Herckes P, Westerhoff P, Kaegi R. Characterization of food-grade titanium dioxide: the presence of nano-sized particles. Environ Sci Technol. 2014;48:6391–400.
5. Bettini S, Boutet-Robinet E, Cartier C, Comera C, Gaultier E, Dupuy J, Naud N, Taché S, Grysan P, Reguer S, Thieriet N, Réfrégiers M, Thiaudière D, Cravedi J-P, Carrière M, Audinot J-N, Pierre FH, Guzylack-Piriou L, Houdeau E. Oral exposure to food-grade TiO_2 impairs intestinal and systemic immune homeostasis and initiates colon carcinogenesis in rats. Sci Rep. 2017;7:40373.
6. Dorier M, Béal D, Marie-Desvergne C, Dubosson M, Barreau F, Houdeau E, Herlin-Boime N, Carrière M. Continuous in vitro exposure of intestinal epithelial cells to E171 food additive causes oxidative stress, inducing oxidation of DNA bases but no endoplasmic reticulum stress. Nanotoxicology. 2017;11:751–61.
7. EFSA Panel on Food Additives and Nutrient Sources Added to Food. Scientific opinion on the re-evaluation of titanium dioxide (E 171) as a food additive. EFSA J. 2016;14:4545.
8. Koeneman BA, Zhang Y, Westerhoff P, Chen Y, Crittenden JC, Capco DG. Toxicity and cellular responses of intestinal cells exposed to titanium dioxide. Cell Biol Toxicol. 2010;26:225–38.
9. Gerloff K, Fenoglio I, Carella E, Kolling J, Albrecht C, Boots AW, Förster I, Schins RP. Distinctive toxicity of TiO_2 rutile/anatase mixed phase nanoparticles on Caco-2 cells. Chem Res Toxicol. 2012;25:646–55.
10. Gerloff K, Pereira DI, Faria N, Boots AW, Kolling J, Förster I, Albrecht C, Powell JJ, Schins RP. Influence of simulated gastrointestinal conditions on

Talbot *et al. J Nanobiotechnol (2018) 16:53*

Page 13 of 14

particle-induced cytotoxicity and interleukin-8 regulation in differenti-
ated and undifferentiated Caco-2 cells. Nanotoxicology. 2013;7:353–66.

11. Faust JJ, Doudrick K, Yang Y, Westerhoff P, Capco DG. Food grade titanium
dioxide disrupts intestinal brush border microvilli in vitro independent of
sedimentation. Cell Biol Toxicol. 2014;30:169–88.

12. Gitrowski C, Al-Jubory AR, Handy RD. Uptake of different crystal
structures of TiO$_2$ nanoparticles by Caco-2 intestinal cells. Toxicol Lett.
2014;226:264–76.

13. Dorier M, Brun E, Veronesi G, Barreau F, Pernet-Gallay K, Desvergne C,
Rabilloud T, Carapito C, Herlin-Boime N, Carrière M. Impact of anatase and
rutile titanium dioxide nanoparticles on uptake carriers and efflux pumps
in Caco-2 gut epithelial cells. Nanoscale. 2015;7:7352–60.

14. Jones K, Morton J, Smith I, Jurkschat K, Harding AH, Evans G. Human
in vivo and in vitro studies on gastrointestinal absorption of titanium
dioxide nanoparticles. Toxicol Lett. 2015;233:95–101.

15. Ruiz PA, Morón B, Becker HM, Lang S, Atrott K, Spalinger MR, Scharl M,
Wojtal KA, Fischbeck-Terhalle A, Frey-Wagner I, Hausmann M, Kraemer T,
Rogler G. Titanium dioxide nanoparticles exacerbate DSS-induced colitis:
role of the NLRP3 inflammasome. Gut. 2017;66:1216–24.

16. Johansson ME, Sjövall H, Hansson GC. The gastrointestinal mucus system
in health and disease. Nat Rev Gastroenterol Hepatol. 2013;10:352–61.

17. Ouwerkerk JP, de Vos WM, Belzer C. Glycobiome: bacteria and mucus at
the epithelial interface. Best Pract Res Clin Gastroenterol. 2013;27:25–38.

18. Tomas J, Wrzosek L, Bouznad N, Bouet S, Mayeur C, Noordine M-L,
Honvo-Houeto E, Langella P, Thomas M, Cherbuy C. Primocolonization is
associated with colonic epithelial maturation during conventionalization.
FASEB J. 2013;27:645–55.

19. Wrzosek L, Miquel S, Noordine M-L, Bouet S, Joncquel Chevalier-Curt
M, Robert V, Philippe C, Bridonneau C, Cherbuy C, Robbe-Masselot C,
Langella P, Thomas M. *Bacteroides thetaiotaomicron* and *Faecalibacterium
prausnitzii* influence the production of mucus glycans and the develop-
ment of goblet cells in the colonic epithelium of a gnotobiotic model
rodent. BMC Biol. 2013;11:61.

20. Da Silva S, Robbe-Masselot C, Ait Belgnaoui A, Mancuso A, Mercade-
Loubière M, Cartier C, Gillet M, Ferrier L, Loubière P, Dague E, Théodorou V,
Mercier-Bonin M. Stress disrupts intestinal mucus barrier in rats via mucin
O-glycosylation shift: prevention by a probiotic treatment. Am J Physiol
Gastrointest Liver Physiol. 2014;307:G420–9.

21. Fröhlich E, Roblegg E. Oral uptake of nanoparticles: human relevance and
the role of in vitro systems. Arch Toxicol. 2016;90:2297–314.

22. Mercier-Bonin M, Despax B, Raynaud P, Houdeau E, Thomas M. Mucus
and microbiota as emerging players in gut nanotoxicology: example of
dietary silver and titanium dioxide nanoparticles. Crit Rev Food Sci Nutr.
2018;58:1023–32.

23. Brun E, Barreau F, Veronesi G, Fayard B, Sorieul S, Chanéac C, Carapito C,
Rabilloud T, Mabondzo A, Herlin-Boime N, Carrière M. Titanium dioxide
nanoparticle impact and translocation through ex vivo, in vivo and
in vitro gut epithelia. Part Fibre Toxicol. 2014;11:13.

24. Teubl BJ, Leitinger G, Schneider M, Lehr CM, Fröhlich E, Zimmer A,
Roblegg E. The buccal mucosa as a route for TiO$_2$ nanoparticle uptake.
Nanotoxicology. 2015;9:253–61.

25. Teubl BJ, Schimpel C, Leitinger G, Bauer B, Fröhlich E, Zimmer A, Roblegg
E. Interactions between nano-TiO$_2$ and the oral cavity: impact of
nanomaterial surface hydrophilicity/hydrophobicity. J Hazard Mater.
2015;286:298–305.

26. Chen EY, Garnica M, Wang YC, Chen CS, Chin WC. Mucin secretion
induced by titanium dioxide nanoparticles. PLoS ONE. 2011;6:e16198.

27. Dudefoi W, Terrisse H, Richard-Plouet M, Gautron E, Popa F, Humbert B,
Ropers MH. Criteria to define a more relevant reference sample of tita-
nium dioxide in the context of food: a multiscale approach. Food Addit
Contam. 2017;34:653–65.

28. Burger-van Paassen N, Vincent A, Puiman PJ, van der Sluis M, Bouma J,
Boehm G, van Goudoever JB, van Seuningen I, Renes IB. The regulation of
intestinal mucin MUC2 expression by short-chain fatty acids: implications
for epithelial protection. Biochem J. 2009;420:211–9.

29. Rasmussen K, Mast J, De Temmerman P-J, Verleysen E, Waege-
neers N, Van Steen F et al. Titanium Dioxide, NM-100, NM-101,
NM-102, NM-103, NM-104, NM-105: characterisation and
physico-chemical properties (JRC). EUR—Scientific and Techni-
cal Research Reports. 2014. https://ec.europa.eu/jrc/en/publicatio
n/eur-scientific-and-technical-research-reports/titanium-dioxi

de-nm-100-nm-101-nm-102-nm-103-nm-104-nm-105-characterisatio
n-and-physico. Accessed 7 May 2018. https://doi.org/10.2788/79554.

30. Jensen KA, Kembouche Y, Christiansen E, Jacobsen NR, Wallin H, Guiot
C, Spalla O, Witschger O. Final protocol for producing suitable manufac-
tured nanomaterial exposure media (Nanogenotox). Report. The generic
NANOGENOTOX dispersion protocol—Standard Operation Procedure
(SOP) and background documentation. 2011.

31. Lesuffleur T, Porchet N, Aubert JP, Swallow D, Gum JR, Kim YS, Real FX,
Zweibaum A. Differential expression of the human mucin genes MUC1
to MUC5 in relation to growth and differentiation of different mucus-
secreting HT-29 cell subpopulations. J Cell Sci. 1993;106:771–83.

32. Turpin W, Humblot C, Noordine M-L, Thomas M, Guyot JP. Lactobacil-
laceae and cell adhesion: genomic and functional screening. PLoS ONE.
2012;7:e38034.

33. Radziwill-Bienkowska JM, Robert V, Drabot K, Chain F, Cherbuy C, Langella
P, Thomas M, Bardowski JK, Mercier-Bonin M, Kowalczyk M. Contribu-
tion of plasmid-encoded peptidase S8 (PrtP) to adhesion and transit in
the gut of *Lactococcus lactis* IBB477 strain. Appl Microbiol Biotechnol.
2017;101:5709–21.

34. Boudjemaa R, Briandet R, Revest M, Jacqueline C, Caillon J, Fontaine-
Aupart M-P, Steenkeste K. New insight into daptomycin bioavailability
and localization in *Staphylococcus aureus* biofilms by dynamic fluores-
cence imaging. Antimicrob Agents Chemother. 2016;8:4983–90.

35. Lan A, Bruneau A, Bensaada M, Philippe C, Bellaud P, Rabot S, Jan G.
Increased induction of apoptosis by *Propionibacterium freudenreichii*
TL133 in colonic mucosal crypts of human microbiota-associated rats
treated with 1,2-dimethylhydrazine. Br J Nutr. 2008;100:1251–9.

36. Rossez Y, Maes E, Lefebvre-Darroman T, Gosset P, Ecobichon C, Joncquel
Chevalier Curt M, Boneca IG, Michalski JC, Robbe-Masselot C. Almost all
human gastric mucin *O*-glycans harbor blood group A, B or H antigens
and are potential binding sites for *Helicobacter pylori*. Glycobiology.
2012;22:1193–206.

37. Proquin H, Rodríguez-Ibarra C, Moonen CG, Urrutia Ortega IM, Briedé
JJ, de Kok TM, van Loveren H, Chirino YI. Titanium dioxide food additive
(E171) induces ROS formation and genotoxicity: contribution of micro
and nano-sized fractions. Mutagenesis. 2017;32:139–49.

38. Urrutia-Ortega IM, Garduño-Balderas LG, Delgado-Buenrostro NL,
Freyre-Fonseca V, Flores-Flores JO, González-Robles A, Pedraza-Chaverri J,
Hernández-Pando R, Rodríguez-Sosa M, León-Cabrera S, Terrazas LI, van
Loveren H, Chirino YI. Food-grade titanium dioxide exposure exacerbates
tumor formation in colitis associated cancer model. Food Chem Toxicol.
2016;93:20–31.

39. Taurozzi JS, Hackley VA, Wiesner MR. Ultrasonic dispersion of nanoparti-
cles for environmental, health and safety assessment-issues and recom-
mendations. Nanotoxicology. 2011;5:711–29.

40. Coconnier MH, Klaenhammer TR, Kernéis S, Bernet MF, Servin AL.
Protein-mediated adhesion of *Lactobacillus acidophilus* BG2FO4 on
human enterocyte and mucus-secreting cell lines in culture. Appl Environ
Microbiol. 1992;58:2034–9.

41. Gouyer V, Wiede A, Buisine M-P, Dekeyser S, Moreau O, Lesuffleur T,
Hoffmann W, Huet G. Specific secretion of gel-forming mucins and TFF
peptides in HT-29 cells of mucin-secreting phenotype. Biochim Biophys
Acta BBA Mol Cell Res. 2001;1539:71–84.

42. Gibbins HL, Proctor GB, Yakubov GE, Wilson S, Carpenter GH. SIgA binding
to mucosal surfaces is mediated by mucin-mucin interactions. PLoS ONE.
2015;10:e0119677.

43. Coïc Y-M, Baleux F, Poyraz Ö, Thibeaux R, Labruyere E, Chretien F, Sobhani
I, Lazure T, Wyplosz B, Schneider G, Mulard L, Sansonetti PJ, Marteyn BS.
Design of a specific colonic mucus marker using a human commensal
bacterium cell surface domain. J Biol Chem. 2012;287:15916–22.

44. Sperandio B, Fischer N, Chevalier-Curt MJ, Rossez Y, Roux P, Robbe Mas-
selot C, Sansonetti PJ. Virulent *Shigella flexneri* affects secretion, expres-
sion, and glycosylation of gel-forming mucins in mucus-producing cells.
Infect Immun. 2013;81:3632–43.

45. Etzold S, Kober OI, MacKenzie DA, Tailford LE, Gunning AP, Walshaw J,
Hemmings AM, Juge N. Structural basis for adaptation of lactobacilli to
gastrointestinal mucus: structure of *Lactobacillus* mucus binding protein.
Environ Microbiol. 2014;16:888–903.

46. Georgantzopoulou A, Serchi T, Cambier S, Leclercq CC, Renaut J, Shao
J, Kruszewski M, Lentzen E, Grysan P, Eswara S, Audinot J-N, Contal S,
Ziebel J, Guignard C, Hoffmann L, Murk AJ, Gutleb AC. Effects of silver

Talbot *et al. J Nanobiotechnol (2018) 16:53*

Page 14 of 14

nanoparticles and ions on a co-culture model for the gastrointestinal epithelium. Part Fibre Toxicol. 2016;13:9.

47. Ermund A, Schütte A, Johansson ME, Gustafsson JK, Hansson GC. Studies of mucus in mouse stomach, small intestine, and colon. I. Gastrointestinal mucus layers have different properties depending on location as well as over the Peyer's patches. Am J Physiol Gastrointest Liver Physiol. 2013;305:G341–7.

48. Johansson MEV, Phillipson M, Petersson J, Holm L, Velcich A, Hansson GC. The inner of the two Muc2 mucin-dependent mucus layers in colon is devoid of bacteria. Proc Natl Acad Sci USA. 2008;105:15064–9.

49. Johansson ME, Larsson JM, Hansson GC. The two mucus layers of colon are organized by the MUC2 mucin, whereas the outer layer is a legislator of host-microbial interactions. Proc Natl Acad Sci USA. 2011;108:4659–65.

50. Kamphuis JBJ, Mercier-Bonin M, Eutamène H, Théodorou V. Mucus organisation is shaped by colonic content; a new view. Sci Rep. 2017;7:8527.

51. Bäckhed F, Ley RE, Sonnenburg JL, Peterson DA, Gordon J. Host-bacterial mutualism in the human intestine. Science. 2005;307:1915–20.

52. Sonnenburg JL, Xu J, Leip DD, Chen CH, Westover BP, Weatherford J, Buhler JD, Gordon JI. Glycan foraging in vivo by an intestine-adapted bacterial symbiont. Science. 2005;307:1955–9.

53. El Kaoutari A, Armougom F, Gordon JI, Raoult D, Henrissat B. The abundance and variety of carbohydrate-active enzymes in the human gut microbiota. Nat Rev Microbiol. 2013;11:497–504.

54. Juge N. Microbial adhesins to gastrointestinal mucus. Trends Microbiol. 2012;20:30–9.

55. Robbe C, Capon C, Coddeville B, Michalski JC. Structural diversity and specific distribution of *O*-glycans in normal human mucins along the intestinal tract. Biochem J. 2004;384:307–16.

56. Png CW, Linden SK, Gilshenan KS, Zoetendal EG, McSweeney CS, Sly LI, McGuckin MA, Florin TH. Mucolytic bacteria with increased prevalence in IBD mucosa augment in vitro utilization of mucin by other bacteria. Am J Gastroenterol. 2010;105:2420–8.

57. Everard A, Belzer C, Geurts L, Geurts L, Ouwerkerk JP, Druart C, Bindels LB, Guiot Y, Derrien M, Muccioli GG, Delzenne NM, de Vos WM, Cani PD. Cross-talk between *Akkermansia muciniphila* and intestinal epithelium controls diet-induced obesity. Proc Natl Acad Sci USA. 2013;110:9066–71.

58. Von Ossowski I, Reunanen J, Satokari R, Vesterlund S, Kankainen M, Huhtinen H, Tynkkynen S, Salminen S, de Vos WM, Palva A. Mucosal adhesion properties of the probiotic *Lactobacillus rhamnosus* GG SpaCBA and SpaFED pilin subunits. Appl Environ Microbiol. 2010;76:2049–57.

59. MacKenzie DA, Jeffers F, Parker ML, Vibert-Vallet A, Bongaerts RJ, Roos S, Walter J, Juge N. Strain-specific diversity of mucus-binding proteins in the adhesion and aggregation properties of *Lactobacillus reuteri*. Microbiology. 2010;156:3368–78.

60. Liu P, Duan W, Wang Q, Li X. The damage of outer membrane of *Escherichia coli* in the presence of TiO$_2$ combined with UV light. Colloids Surf B Biointerfaces. 2010;78:171–6.

61. Kumar A, Pandey AK, Singh SS, Shanker R, Dhawan A. Engineered ZnO and TiO(2) nanoparticles induce oxidative stress and DNA damage

leading to reduced viability of *Escherichia coli*. Free Radic Biol Med. 2011;51:1872–81.

62. Zhukova LV, Kiwi J, Nikandrov VV. TiO$_2$ nanoparticules suppress *Escherichia coli* cell division in the absence of UV irradiation in acidic conditions. Colloids Surf B Biointerfaces. 2012;97:240–7.

63. Radziwill-Bienkowska JM, Talbot P, Kamphuis JBJ, Robert V, Cartier C, Fourquaux I, Lentzen E, Audinot J-N, Jamme F, Réfrégiers M, Bardowski JK, Langella P, Kowalczyk M, Houdeau E, Thomas M, Mercier-Bonin M. Toxicity of food-grade TiO$_2$ to commensal intestinal and transient food-borne bacteria: new insights using Nano-SIMS and synchrotron UV fluorescence imaging. Front Microbiol. 2018;9:1–14.

64. Claus SP, Guillou H, Ellero-Simatos S. The gut microbiota: a major player in the toxicity of environmental pollutants? Npj Biofilms Microbiomes. 2016;2:16003.

65. Ribière C, Peyret P, Parisot N, Darcha C, Déchelotte PJ, Barnich N, Peyretaillade E, Boucher D. Oral exposure to environmental pollutant benzo[a]pyrene impacts the intestinal epithelium and induces gut microbial shifts in murine model. Sci Rep. 2016;6:31027.

66. Jin Y, Wu S, Zeng Z, Fu Z. Effects of environmental pollutants on gut microbiota. Environ Pollut. 2017;222:1–9.

67. Fröhlich EE, Fröhlich E. Cytotoxicity of nanoparticles contained in food on intestinal cells and the gut microbiota. Int J Mol Sci. 2016;17:509.

68. Pietroiusti A, Magrini A, Campagnolo L. New frontiers in nanotoxicology: gut microbiota/microbiome-mediated effects of engineered nanomaterials. Toxicol Appl Pharmacol. 2016;299:90–5.

69. Barcelo A, Claustre J, Moro F, Chayvialle JA, Cuber JC, Plaisancie P. Mucin secretion is modulated by luminal factors in the isolated vascularly perfused rat colon. Gut. 2000;46:218–24.

70. Gaudier E, Jarry A, Blottière HM, de Coppet P, Buisine MP, Aubert JP, Laboisse C, Cherbut C, Hoebler C. Butyrate specifically modulates MUC gene expression in intestinal epithelial goblet cells deprived of glucose. Am J Physiol Gastrointest Liver Physiol. 2004;287:G1168–74.

71. Gaudier E, Rival M, Buisine MP, Robineau I, Hoebler C. Butyrate enemas upregulate Muc genes expression but decrease adherent mucus thickness in mice colon. Physiol Res. 2009;58:111–9.

72. Belzer C, De Vos WM. Microbes inside—from diversity to function: the case of *Akkermansia*. ISME J. 2012;6:1449–58.

73. Tremaroli V, Backhed F. Functional interactions between the gut microbiota and host metabolism. Nature. 2012;489:242–9.

74. Van den Abbeele P, Belzer C, Goossens M, Kleerebezem M, De Vos WM, Thas O, De Weirdt R, Kerckhof FM, Van de Wiele T. Butyrate-producing *Clostridium* cluster XIVa species specifically colonize mucins in an in vitro gut model. ISME J. 2013;7:949–61.

75. Jeong GN, Jo UB, Ryu HY, Kim YS, Song KS, Yu IJ. Histochemical study of intestinal mucins after administration of silver nanoparticles in Sprague-Dawley rats. Arch Toxicol. 2010;84:63–9.